Matter and Radiation at Extremes

REVIEW ARTICLE | MAY 25 2018

Collimated gamma rays from laser wakefield accelerated electrons

Minghua Li; Liming Chen ✉; Dazhang Li; Kai Huang; Yifei Li; Yong Ma; Wenchao Yan; Mengze Tao; Junhao Tan; Zhengming Sheng; Jie Zhang

Check for updates

Matter Radiat. Extremes 3, 188–196 (2018)
https://doi.org/10.1016/j.mre.2018.03.002

CrossMark
View Online
Export Citation

23 November 2023 14:53:30

AIP Publishing

MATTER AND RADIATION AT EXTREMES

Matter and Radiation at Extremes 3 (2018) 188–196

Review article

Collimated gamma rays from laser wakefield accelerated electrons

Minghua Li [a], Liming Chen [a,b,c,*], Dazhang Li [d], Kai Huang [a,e], Yifei Li [a], Yong Ma [a], Wenchao Yan [a], Mengze Tao [a], Junhao Tan [a], Zhengming Sheng [c,f,g], Jie Zhang [c,f]

[a] *Beijing National Laboratory of Condensed Matter Physics, Institute of Physics, Chinese Academy of Sciences, Beijing 100190, China*
[b] *School of Physical Sciences, University of Chinese Academy of Sciences, Beijing 100190, China*
[c] *IFSA Collaborative Innovation Center, Shanghai Jiao Tong University, Shanghai 200240, China*
[d] *Institute of High Energy Physics, Chinese Academy of Sciences, Beijing 100049, China*
[e] *Kansai Photon Science Institute (KPSI), National Institutes for Quantum and Radiological Science and Technology (QST), 8-1-7 Umemidai, Kizugawa, Kyoto 619-0215, Japan*
[f] *Key Laboratory for Laser Plasmas (MOE) and Department of Physics and Astronomy, Shanghai Jiao Tong University, Shanghai 200240, China*
[g] *SUPA, Department of Physics, University of Strathclyde, Glasgow G4 0NG, United Kingdom*

Received 22 January 2018; accepted 14 March 2018
Available online 25 May 2018

Abstract

Betatron radiation from laser wakefield accelerated electrons and X-rays scattered off a counter-propagating relativistic electron bunch are collimated and hold the potential to extend the energy range to hard X-ray or gamma ray band. The peak brightness of these incoherent radiations could reach the level of the brightest synchrotron light sources in the world due to their femtosecond pulse duration and source size down to a few micrometers. In this article, the principle and properties of these radiation sources are briefly reviewed and compared. Then we present our recent progress in betatron radiation enhancement in the perspective of both photon energy and photon number. The enhancement is triggered by using a clustering gas target, arousing a second injection of a fiercely oscillating electron bunch with large charge or stimulating a resonantly enhanced oscillation of the ionization injected electrons. By adopting these methods, bright photon source with energy over 100 keV is generated which would greatly impact applications such as nuclear physics, diagnostic radiology, laboratory astrophysics and high-energy density science.
© 2018 Science and Technology Information Center, China Academy of Engineering Physics. Publishing services by Elsevier B.V. This is an open access article under the CC BY-NC-ND license (http://creativecommons.org/licenses/by-nc-nd/4.0/).

PACS codes: 52.38.Ph; 52.38.Kd; 52.59.Px

Keywords: Laser wakefield accelerator; Gamma ray; Hard X-ray; Betatron radiation; Enhancement

1. Introduction

As a noxious co-product of the electron accelerators in its early years, synchrotron radiation has now dominated science and industry worldwide. The synchrotron light sources provide X-ray pulses with the merits of tunable energy, high brightness, good collimation and polarization, etc., which make synchrotron radiation a premier choice to probe the structure and dynamics of matter. Despite the unprecedented capability as a research tool, the accelerator based light sources are still developing rapidly towards ultrashort (femtosecond) pulse duration, higher energy (hard X-ray) and higher brightness. Representing the state-of-art light source, the X-ray free electron lasers (XFEL) could deliver coherent X-rays with peak brightness ten orders of magnitude to the 3rd generation light sources, enabling accurate pump-probe measurement of matter in extreme conditions. To meet the enormous need from science community and industry, currently many countries are

* Corresponding author. Institute of Physics, Chinese Academy of Sciences, 8 NanSanJie, Haidian, Beijing 100190, China. Fax: +86 10 82649318.
E-mail address: lmchen@iphy.ac.cn (L. Chen).

https://doi.org/10.1016/j.mre.2018.03.002
2468-080X/© 2018 Science and Technology Information Center, China Academy of Engineering Physics. Publishing services by Elsevier B.V. This is an open access article under the CC BY-NC-ND license (http://creativecommons.org/licenses/by-nc-nd/4.0/).

23 November 2023 14:53:30

developing the fourth generation light source and almost all 3rd generation sources are being upgraded or planned to be upgraded.

Though going through fast expansion, the limited access to these giant machines will definitely slow the pace of science and compromise the quality of research. To reduce the cost and shrink the large scale facility into a university laboratory scale system would benefit scientific researchers all over the world. As complementary methods, compact X-ray light sources (CXLS) would fill the capability gaps in multi disciplines. For this purpose, several CXLS schemes or concepts were proposed and studied. Among those schemes, light sources based on a compact storage ring [1,2] or a conventional undulator [3] are combination of optical methods and conventional accelerator technologies. More concise schemes are based on a laser plasma accelerator (LPA) [4,5] which was first proposed by Tajima and Dawson in 1979 [6]. And LPAs based state-of-the-art X-ray FELs are under extensive study, the discipline has been discussed and several mechanisms have been proposed [1–3]. After development over three decades, different LPA regimes have been proposed and investigated extensively, keeping pace with the available laser systems, i.e. plasma beat wave accelerator (PBWA) [4,5], laser wakefield accelerator (LWFA) [6], self-modulated laser wakefield accelerator [7,8]. However, currently, most LPAs are now working in the so called "bubble" regime [7,8] in which an intense femtosecond laser pulse expels the electrons off the axis of propagation, forming an electron-free cavity which then capture and accelerate electrons to GeV range [9,10]. Lu et al. [9] pointed out that, in the high intensity limit ($a_0 \geq 4$), the bubble will be driven efficiently when the laser spot size r_0 satisfies $k_p r_0 \approx 2\sqrt{a_0}$, while the plasma wave simply presents a sinusoidal form in the mildly relativistic regime, where k_p is the wavenumber of electron plasma wave and a_0 the normalized laser vector potential. In all optical schemes, the laser plasma accelerated electrons are wiggled either in the ion cavity itself (betatron radiation) or in a counter-propagating laser pulse (relativistic Thomson backscattering or Inverse Compton Scattering, ICS), emitting synchrotron radiations like X-rays with approximately the same pulse duration to the drive laser pulse (20–40 fs). Besides the low cost, compactness, micron scale source size and ultrashort pulse duration, these two methods could deliver photons with energy extending to the gamma ray range, this is beyond the reach of the conventional synchrotrons and distinguishes them from the laser driven high harmonic generation (HHG) source which up-converts the laser to extreme ultraviolet (EUV) or soft X-ray regime [11]. Another feature of betatron and ICS source is that the radiation is highly directed, which is different from the case of Kα source [12–14] and LPA based bremsstrahlung [15]. The Kα source typically diverges over all space and the LPA based bremsstrahlung source has a divergence angle of a few degrees (FWHM), while betatron and ICS sources have typically a few mrad. Naturally synchronized with the drive laser pulse along with all the merits mentioned above, betatron and ICS sources are very promising for many interesting applications, including pump-probe study of ultrafast chemical, biological process [10,11], industry and defense sectors [12]. For more detailed applications, we refer the reader to the review of Chen et al. [13].

Two critical factors of the light source for application are the operation energy range and photon flux. We have been studying laser driven secondary sources for decades with laser systems of different scale and parameters, and have achieved progress in enhancing the betatron radiation both in photon energy and flux recently. By using a clustering gas jet, direct laser acceleration (DLA) mechanism is stimulated, causing much more electrons to be accelerated and wiggled with large amplitude, hence more photons are emitted [16]. Another method to achieve large charge and wiggle amplitude is to trigger a continuously injected electron bunch through the laser and bubble evolution [17,18]. Finally, the electron transverse oscillation could also be enhanced via the ionization injected electrons resonating with the drive laser pulse [19]. These progresses make laser based betatron radiation more efficient and pave the way for applications.

In this article, we review the betatron radiation and ICS sources from laser plasma accelerators in Section 2. As radiation originated from accelerated charge, they are analogous to the synchrotron radiation. In Sections 3, 4 and 5, we summarize our recent progresses in betatron enhancement.

2. All optical LPA based collimated gamma ray sources

2.1. Radiation of a relativistically moving electron

In the framework of classical electrodynamics, the very essence of betatron radiation and ICS is just like the synchrotron radiation. In order to characterize the radiation features of betatron and ICS, the radiation of a relativistic moving electron is reviewed briefly. Consider an electron moving relativistically ($\gamma \gg 1$) in an arbitrary orbit $\boldsymbol{r}(t)$, the radiated energy per unit solid angle and per unit frequency interval is [20].

$$\frac{\mathrm{d}^2 I}{\mathrm{d}\omega \mathrm{d}\Omega} = \frac{e^2}{4\pi^2 c}\left| \int_{-\infty}^{\infty} \frac{\boldsymbol{n}\times\left[(\boldsymbol{n}-\boldsymbol{\beta})\times\dot{\boldsymbol{\beta}}\right]}{(1-\boldsymbol{\beta}\cdot\boldsymbol{n})^2} \exp\{\mathrm{i}\omega[t-\boldsymbol{n}\times\boldsymbol{r}(t)/c]\}\mathrm{d}t \right|^2. \tag{1}$$

Here $\boldsymbol{n}$ is the direction of observation, $\boldsymbol{\beta}$ and $\dot{\boldsymbol{\beta}}$ are the velocity and acceleration which could be derived from a known $\boldsymbol{r}$ (t). It shows clearly that the acceleration is essential for radiation. More detailed analysis shows $P \propto \boldsymbol{F}_{\parallel}^2$ and $P \propto \gamma^2 \boldsymbol{F}_{\perp}^2$ [21], i.e., transverse force ($\boldsymbol{F} \perp \boldsymbol{\beta}$) is much more efficient for driving this radiation. The radiation features are directly linked to the electron orbit, which results in two distinct regimes depending on the relationship of the radiation opening angle $(1/\gamma)$ and the maximum angle $(\theta_{\max})$ of the trajectory to the propagation axis. When $\theta_{\max} \ll 1/\gamma$, the radiation from different parts of the trajectory is directed along the propagation axis, corresponding to the undulator regime; When $\theta_{\max} \gg 1/\gamma$, the other regime called wiggler regime dominates. Now a very important parameter called strength

23 November 2023 14:53:30

parameter is defined as $K = \gamma\theta_{\max}$, which differs the undulator regime from wiggler regime. For instantaneously circular motion, Eq. (1) becomes [20].

$$\frac{\mathrm{d}^2 I}{\mathrm{d}\omega \mathrm{d}\Omega} = \frac{e^2}{3\pi^2 c}\left(\frac{\omega\rho}{c}\right)^2\left(\frac{1}{\gamma^2}+\theta^2\right)^2\left[K_{2/3}^2(\xi) + \frac{\theta^2}{1/\gamma^2+\theta^2}K_{1/3}^2(\xi)\right], \tag{2}$$

where $\xi = (\omega\rho/3c)(1/\gamma^2+\theta^2)^{3/2}$ and ρ is the curvature radius of the orbit; $K_{1/3}^2(\xi)$, $K_{2/3}^2(\xi)$ are the modified Bessel functions, which become negligible for $\xi \gg 1$. Applying sinusoidal approximation, with an oscillation period λ_{osc}, the fundamental frequency is given by

$$\omega = \frac{4\pi\gamma^2 c}{\lambda_{\mathrm{osc}}}\left(1+\frac{K^2}{2}+\gamma^2\theta^2\right)^{-1}. \tag{3}$$

For $K \ll 1$ (undulator regime), the electron radiates only at the fundamental frequency, with K approaching unity, harmonics appears. When $K \gg 1$ (wiggler regime), the radiation contains harmonics extending to the critical frequency ω_{c}, which is defined at $\xi = 1/2$ (the modified Bessel functions are still appreciable) and $\theta = 0$,

$$\omega_{\mathrm{c}} = \frac{3c}{2\rho}\gamma^3. \tag{4}$$

For a sinusoidal orbit, the critical frequency goes to $\omega_{\mathrm{c}} = 3K\pi c\gamma^2/\lambda_{\mathrm{u}}$, at extremum of the orbit, where λ_{u} denotes the sinusoidal orbit period. Beyond the critical frequency, the radiation decreases exponentially. The radiation power below ω_{c} equals the radiation power above ω_{c}. Integrating over all angles, Eq. (2) becomes

$$\frac{\mathrm{d}I}{\mathrm{d}\omega} = \sqrt{3}\,\frac{e^2}{c}\gamma\frac{\omega}{\omega_{\mathrm{c}}}\int_{\omega/\omega_{\mathrm{c}}}^{\infty} K_{5/3}(x)\mathrm{d}x. \tag{5}$$

Eq. (5) divided by $\hbar\omega$ gives the distribution of photon number

$$\frac{\mathrm{d}N}{\mathrm{d}E} = \frac{9\sqrt{3}I}{8\pi E_{\mathrm{c}}^2}\int_{E/E_{\mathrm{c}}}^{\infty} K_{5/3}(x)\mathrm{d}x, \tag{6}$$

where $E_{\mathrm{c}} = \hbar\omega_{\mathrm{c}}$ is the critical energy and $I = 4\pi e^2\gamma^4/3\rho = 8\pi e^2\gamma\omega_{\mathrm{c}}/9c$ is the total radiation energy per period. The integration of Eq. (6) gives the photon number emitted per electron per period for wiggler regime

$$N = \frac{5\pi}{\sqrt{3}}\alpha K, \tag{7}$$

where $\alpha = e^2/\hbar c = 1/137$ is the fine structure constant, N divided by I gives the mean photon energy

$$\overline{E} = \frac{8}{15\sqrt{3}}E_{\mathrm{c}} \approx 0.3E_{\mathrm{c}}. \tag{8}$$

While for the undulator regime, the photon number goes to

$$N = \frac{2\pi}{3}\alpha K^2. \tag{9}$$

For all the cases discussed in this article, the radiation from an electron bunch with N_{e} electrons could be incoherently summed, i.e., the total photon number $N_{\mathrm{total}} = N_{\mathrm{osc}}N_{\mathrm{e}}N$ with N_{osc} the number of oscillation periods. While for the case of FEL, the radiation of microbunched electrons is summed coherently, i.e., the total photon number is proportional to N_{e}^2.

2.2. Betatron radiation from LPA

Betatron radiation from electrons undergoing transverse oscillation while being accelerated in the bubble is analogous to the synchrotron radiation in the wiggler regime, i.e., the bubble acts both as the accelerator and undulator. Esarey et al. investigated and characterized the radiation from electron beams in plasma channels [22]. Betatron radiation from laser plasma interaction is first demonstrated experimentally in 2004 [23], since then great progress has been made [19,24,25], applications with these sources have been evaluated and carried out [25–28].

From the analysis in Subsection 2.1, the general idea to address the radiation properties is to start with the electron trajectory which leads to the strength parameter K and radiation frequency. Here the blow-out (bubble) model is used for the laser plasma accelerator [7]. Consider an ion sphere cavity of radius $r_{\mathrm{b}} = 2c\sqrt{a_0}/\omega_{\mathrm{p}}$, the equation of motion for a test electron in the ion cavity can be derived via the electromagnetic field distribution. From the equation of motion the betatron oscillation frequency is obtained, which is $\omega_\beta = \omega_{\mathrm{p}}/\sqrt{2\gamma}$. Here $\omega_{\mathrm{p}} = (4\pi e^2 n_{\mathrm{e}}/m_{\mathrm{e}})^{1/2}$ is the plasma frequency and $a_0 = eA/m_{\mathrm{e}}c^2 \approx 0.85\times10^{-9}I^{1/2}[\mathrm{W\cdot cm^{-2}}]\lambda[\mu\mathrm{m}]$ is the normalized laser vector potential. The betatron frequency corresponds to the electron oscillation frequency in Subsection 2.1, i.e., the oscillation period in Eq. (3) goes to

$$\lambda_\beta = 2\pi c/\omega_\beta = \sqrt{2\gamma}\lambda_{\mathrm{p}}. \tag{10}$$

For an electron orbit with oscillation amplitude r_β, the strength parameter K goes to

$$K = \gamma\theta_{\max} \approx \gamma r_\beta k_\beta = r_\beta k_{\mathrm{p}}\sqrt{\gamma}\Big/\sqrt{2}. \tag{11}$$

For small amplitude oscillation ($K \ll 1$), the radiation is analogous to the synchrotron radiation in the undulator regime. The fundamental frequency is given by Eq. (3) together with the betatron period given by Eq. (10).

For $K \gg 1$, the electrons emit harmonics extending to the critical frequency given by Eq. (4). The minimum curvature radius for a sinusoidal obit is obtained at the crest or trough of the orbit, which is $\rho_{\min} = 1/r_\beta k_\beta^2 = \gamma\lambda_\beta/2\pi K$. Together with Eq. (9), the critical frequency is obtained as

$$\omega_{\mathrm{c}} = 3c\pi^2\gamma^2\frac{r_\beta}{\lambda_{\mathrm{p}}^2}. \tag{12}$$

23 November 2023 14:53:30

The photon number emitted is given by Eq. (7), which is only related to the strength parameter K. From Eq. (11), it is clear that the strength parameter is determined by the oscillation amplitude, electron energy and electron density. Based on the recent development of LPAs and both our experimental and numerical researches, realistic and typical laser and electron parameters within the bubble regime are given to perform primary estimation of the betatron radiation.

First we consider a 20 TW Ti:sapphire laser which delivers 500 mJ to a 1.2 mm gas jet with 25 fs pulse duration, the normalized vector potential is $a_0 = 1.5$. With a plasma density of $n_e = 5 \times 10^{18}\,\mathrm{cm}^{-3}$, we have $\lambda_p = 14.9\,\mu\mathrm{m}$ and $r_b = 5.8\,\mu\mathrm{m}$. The monoenergetic electron bunch peaked at 100 MeV ($\gamma = 200$) contains 1.2×10^8 electrons (~20 pC). The betatron oscillation period is $\lambda_\beta = 298\,\mu\mathrm{m}$. Assuming $r_\beta = 3\,\mu\mathrm{m}$, we have $K = 12.6$ and $\hbar\omega_c = 3.1$ keV. With the number of betatron oscillation periods $N_\beta \sim L/\lambda_\beta = 4$, the total emitted photon number is $N_{\mathrm{total}} = N_\beta N_e N \approx 4 \times 10^8$, here L is the interaction length [22]. The photon number with energy above 10 keV is 4.7×10^6.

100 TW class laser systems are also widely used in the LPA community. These lasers typically deliver a few joules energy in a few tens femtoseconds, e.g., 3 J in 30 fs. Setting $a_0 = 2$ and $n_e = 1 \times 10^{19}\,\mathrm{cm}^{-3}$, we have $\lambda_p = 10.6\,\mu\mathrm{m}$ and $r_b = 4.7\,\mu\mathrm{m}$. 300 MeV ($\gamma = 600$), 50 pC electron beam could be expected with an acceleration length of 3 mm [29]. Still take the oscillation amplitude to be 3 μm, we have $\lambda_\beta = 366\,\mu\mathrm{m}$, $K = 31$ and $\hbar\omega_c = 56.6$ keV. The total photon number is then derived to be $N_{\mathrm{total}} = N_\beta N_e N \approx 2.5 \times 10^9$. The photon number with energy above 50 keV and 100 keV is 4.3×10^8 and 1.3×10^8 respectively.

As the laser power goes up to the petawatt regime, the interaction could be very different from the blow-out regime. These PW facilities deliver multi-kilojoule picosecond pulses. The pulses have durations longer than the plasma period, resulting in the self-modulated LWFA (SM-LWFA) or DLA scenario. In SM-LWFA and DLA regime, the continuously injected and accelerated electrons execute betatron oscillation with larger amplitude. The electron bunch has charge up to several tens of nanocoulombs, though 100% energy spread and large divergence [30,31]. The X-ray photon number with energy of a few tens keV is over 1×10^{11}. However, for proper parameters (lower plasma density), the blow-out regime dominates the interaction. GeV, nC electron bunch could be obtained, $\sim 2 \times 10^9$ photons are emitted with critical energy about 10 keV [31].

By using different techniques, brighter and harder betatron photon sources could be realized, e.g., bright gamma ray with critical energy ~ 1.2 MeV, which we will present in the following sections.

2.3. Relativistic Thomson backscattering sources

For the betatron radiation sources, the ion cavity acts as both accelerator and wiggler. While in this subsection we will discuss radiation from pre-accelerated relativistic electrons oscillating in a counter-propagating laser pulse, i.e., an electromagnetic undulator. This radiation process is simply Thomson scattering in the rest frame of the relativistically moving electrons, but the photon energy is upshifted in the laboratory frame. Also known as the Inverse Compton Scattering (ICS), this process is also analogous to synchrotron radiation. Different from betatron and conventional undulator, this electromagnetic undulator has much shorter period which leads to higher radiation frequency. As a promising scheme for realizing bright gamma ray source, the ICS source has been investigated both theoretically [32–34] and experimentally [29,35–39]. Multi-MeV gamma rays with $\sim 10^7$ photons are generated from the collision of the LPA electrons with the colliding laser pulse.

Radiation properties of the ICS can readily be derived from the formulas in Subsection 2.1. The oscillation period is $\lambda_{\mathrm{osc}} = \lambda_{\mathrm{laser}}/2$ and the strength parameter is given by $K = a_0$. For linear Thomson scattering which corresponds to the undulator regime ($K < 1$), the radiation is at the fundamental frequency given by ($\theta = 0$)

$$\omega = \frac{8\pi\gamma^2 c}{\lambda_{\mathrm{laser}}}\left(1 + \frac{a_0^2}{2}\right)^{-1}. \tag{13}$$

Photon number emitted by an electron integrating over all angles is given by Eq. (9). For an electron bunch with N_e electrons oscillating in a counter-propagating laser pulse with pulse duration of τ, the total photons emitted is given by

$$N_{\mathrm{total}} = \frac{4\pi c\tau}{3\lambda_{\mathrm{laser}}}\alpha N_e a_0^2. \tag{14}$$

The opening angle of the radiation is $1/\gamma$ and the line width of the emission is $\Delta\lambda/\lambda = \lambda_{\mathrm{laser}}/2c\tau$.

Electrons start emitting harmonics when $K \sim 1$. For $K \gg 1$, the scattering goes into the nonlinear regime, corresponding to the wiggler regime of the synchrotron. The critical frequency and total emitted photon number are given by

$$\omega_c = 6\pi c a_0 \gamma^2 / \lambda_{\mathrm{laser}}, N_{\mathrm{total}} = \frac{10\pi c\tau}{\sqrt{3}\lambda_{\mathrm{laser}}}\alpha N_e a_0. \tag{15}$$

The general idea of the ICS source based on LPA is to utilize a second laser pulse colliding with the laser plasma accelerated electron bunch. This scheme owns the advantage in controlling the parameters of the electromagnetic undulator, hence the radiation properties. However, to realize efficient temporal synchronization and spatial overlapping is difficult. In 2012, Ta Phuoc et al. proposed and demonstrated another scheme by using only one laser pulse as both LPA drive pulse and colliding pulse [38]. This is realized by combining the LPA and a relativistic plasma mirror (PM). The laser pulse hit the PM placed at the exit of the gas jet after driving the electron acceleration, reflected by the PM and then collides with the accelerated electron bunch. The advantage of the PM scheme is obvious and attractive: simplicity. By using this simple method, monochromatic gamma rays with photon energy of multi-keV to over MeV are generated and the emitted photon number is over 10^7 [29]. Hai-En Tsai et al.

23 November 2023 14:53:30

characterized the spent drive laser and the performance of the PM [39].

As we did for the betatron radiation, the performance of the ICS source using PM scheme is evaluated by adopting realistic parameters based on experiments and simulations. The drive laser and LPA parameters are chosen to be almost the same with those from Subsection 2.2, while the spent laser and colliding pulse are determined based on the scaling and measurement from Ref. [39].

For the 20 TW (500 mJ, 25 fs) case, the initial normalized laser potential vector is 1.5 ($1/e^2$ spot size $w_0 \sim 10$ μm containing ~75% pulse energy) and the plasma density is $n_e = 5 \times 10^{18}$ cm^{-3}. The charge and peak energy of the electron bunch are 20 pC and 100 MeV. The intensity of the spent laser is estimated to be 3.1×10^{18} W·cm^{-2} and the reflectivity of the PM is 80%, resulting in a colliding pulse with $a_0 \approx 0.95$. The scattering is within the domain of linear scattering, meaning the emitted photons are mainly at fundamental frequency given by Eq. (13). The spectrum is peaked at 135 keV. Assuming that the colliding pulse has the same pulse duration with the drive pulse, the total photon number is calculated to be $N_{\text{total}} \approx 3.24 \times 10^7$.

For the 100 TW laser case, we have $\tau = 30$ fs, $w_0 \sim 25$ μm and $a_{0-\text{drive}} = 2.2$. The plasma density is $n_e = 1 \times 10^{19}$ cm^{-3}. Electron bunch with 50 pC and peaked at 320 MeV is expected. The intensity of the spent laser is $\sim 7 \times 10^{18}$W·cm^{-2} and the PM reflectivity drops to 60%, corresponding to a colliding pulse with $a_0 \approx 1.1$. The interaction here belongs to weakly nonlinear regime and the spectrum is analogous to synchrotron radiation spectrum with a critical energy $\hbar\omega_c \approx 2.1$ MeV. The total photon number with mean photon energy $0.3\hbar\omega_c \approx 630$ keV is $N_{\text{total}} \approx 5.12 \times 10^8$.

To further exploit the potential of LPA-PM ICS sources, we propose to focus the colliding pulse with the PM itself. Recent research shows that the relativistic PM could focus the reflected laser pulse via the laser induced curvature [40]. Nakatsutsumi et al. employed an ellipsoidal shaped plasma mirror to achieve a fivefold (4.4 μm–0.9 μm) reduction of the spot size [41]. By using well designed optics and proper parameters, the reflected pulse will be focused and the intensity will be boosted which will leads to higher nonlinearity. In the framework of quantum electrodynamics, this corresponds to the multi-photon scattering process and enhancement of scattering cross section [42–44]. As an example, let's reconsider the radiation with a 20 TW laser. Supposing a magnification of $w_f/w_i = 0.5$ is achieved, where w_f is the size of focal spot after PM and $w_i \sim \sqrt{2}w_0$ is the beam size at the PM, the focal spot size is $w_f \sim 7$ μm which is close to the optimal spot size according to previous research [45]. The colliding pulse is then busted to $a_0 \approx 3.8$. Adopting the nonlinear limit, the emission spectrum is broadened and hardened. With a critical energy $\hbar\omega_c \approx 706.8$ keV, the total photon number with mean energy $0.3\hbar\omega_c \approx 212$ keV is $N_{\text{total}} \approx 5.89 \times 10^8$. The results show that one can obtain radiation which could only be produced with more powerful lasers due to the high efficiency in using the spent laser energy.

2.4. Discussion and perspectives

In the previous sections we have reviewed the principle of the LPA-based betatron radiation and ICS sources in the framework of classical electrodynamics. Both of betatron and ICS are able to produce high flux gamma rays. Their performances are evaluated under different laser conditions. The parameters of LPA and radiation driven by 20 TW and 100 TW lasers are summarized in Table 1. The differences of these two kinds of radiation sources are obvious. Firstly, the ICS radiation is harder than the betatron radiation. This is because the oscillation period of the ICS is much (~3 orders of magnitude) smaller than the betatron period. Secondly, the betatron radiation is analogous to the synchrotron radiation in the wiggler regime which is featured a continuous spectrum. While for the linear Thomson scattering, monochromatic radiation is possible if the electrons are monochromatic.

These differences and features make betatron and ICS sources suitable for different applications. For ultrafast time-resolved X-ray absorption spectroscopy (XAS) studies, a continuous X-ray source at keV range is needed [46]. The betatron radiation with a 20 TW laser is just perfect for that. Another very important application with this type of source is phase contrast imaging due to the micron size of source and suitable photon energy [27]. For medical applications such as mammography and angiography, the betatron radiation from a 100 TW laser system could be used as it can provide intense X-rays at a few tens keV [47]. The ICS radiation could be applied to gamma ray radiology, industry inspection and weapon storage inspection. The ICS source with MeV range photon energy fits for nuclear physics [48] and pair production which require photon energy higher than twice the rest mass of electron.

Though these innovative laser based sources are very promising, there are still gaps towards efficient application. A major limit of these sources for application is the photon flux. The method mentioned in Subsection 2.3 is one of many possible ways to enhance the performance of these light sources. Moreover, the development of high repetition rate high power laser would boost the photon flux orders of magnitude, making applications easier and more efficient. In the following sections, we will summarize our recent progress in enhancing the betatron radiation.

Table 1
Parameters of LPA based betatron and ICS sources.

Parameter	20 TW (0.5 J, 25 fs)		100 TW (3 J, 30 fs)	
	Betatron	ICS	Betatron	ICS
Electron bunch charge	20 pC	20 pC	50 pC	50 pC
Electron peak energy	100 MeV	100 MeV	300 MeV	320 MeV
Oscillation period	298 μm	0.4 μm	366 μm	0.4 μm
Number of oscillation periods	4	19	8	23
Strength parameter	12.6	0.95	31	1.1
Photon energy	3.1 keV[a]	135 keV	56.6 keV[a]	2.1 MeV[a]
Photon number per pulse	4×10^8	3.2×10^7	2.5×10^9	5.1×10^8

[a] Critical energy $\hbar\omega_c$ for a synchrotron-like spectrum.

23 November 2023 14:53:30

3. Enhancing betatron radiation via clustering gas target

According to the analysis in Section 2, several parameters could be optimized to achieve higher photon yield such as the electron beam charge, the betatron oscillation amplitude and the interaction length. Recently, we succeeded in obtaining much higher electron beam charge and larger betatron oscillation by simply using a clustering gas jet which was formed while gas atoms or molecules with high stagnation expanding into vacuum and holding together by the van der Waals force. By adopting this new method, 2×10^8 photons were emitted driven by a laser with only 3 TW power [16].

The experiment was performed at the XL-II laser facility in the Institute of Physics, Chinese Academy of Sciences. The laser delivers 300 mJ, 80 fs high contrast pulses to be focused into a gas jet which has a 1.2 mm × 10 mm rectangular nozzle at the exit. The laser pulse was focused with an *f*/6 off-axis parabola (OAP) onto a focal spot size of 4±0.1 μm forming an average intensity of 3.0×10^{18} W·cm^{-2} in the focal region. Aside from the argon clustering gas jet with a plasma density of 2×10^{19} cm^3, the pure helium gas jet with the same plasma density was also used for comparison. The resulting electron beam charge was 200 pC with a continuous spectrum extending to over 20 MeV, while for the pure helium gas it was 4 pC and the monochromatic spectrum peaked at 21 MeV. The beam divergence angles for argon and helium are 17 mrad and 1 mrad respectively, indicating large transverse oscillation amplitude. The measured X-ray emission is fitted with a synchrotron radiation spectrum with a critical energy of 0.6 keV. The photon number for the clustering gas target is 2×10^8. This is over one order of magnitude higher than the case with pure helium gas target. These results were obtained only with a high contrast laser (~10^9), because the pre-pulse would cause pre-expansion of the solid density cluster which would cause inefficient heating and acceleration.

Two-dimensional particle-in-cell (PIC) simulation was performed to figure out how the cluster affects the interaction. Fig. 1(a) shows the trajectories of traced electrons for both Ar and He. For Ar clustering gas, the transverse oscillation amplitude increase to 10 μm rapidly. While for the pure He the electron transverse oscillation is mild. The simulation results indicate that the DLA mechanism is responsible for this enhancement. The strong resonant heating of cluster electrons in the beginning of the interaction leads to higher local electron density and a larger pre-acceleration phase in the transverse direction [49], which then leads to efficient acceleration via strong $\boldsymbol{v} \times \boldsymbol{B}$ force and larger amplitude oscillation. Fig. 1(b) and (c) shows the energy gains of electrons from DLA and electrostatic field, 76% of the energy gain is from DLA for the Ar case while it is just 1.35% for pure He gas. As we mentioned in Section 2, the DLA regime is usually encountered when PW lasers are used, but our results show that the DLA mechanism could be stimulated even with modest power laser if the clustering gas target is used.

4. Enhancing betatron radiation via hosing evolution

Our previous research has observed monoenergetic electron beams and bright betatron X-rays simultaneously in one single shot [17], a second continuously injected electron bunch with ~0.1 nC charge and 9 μm oscillation amplitude is

23 November 2023 14:53:30

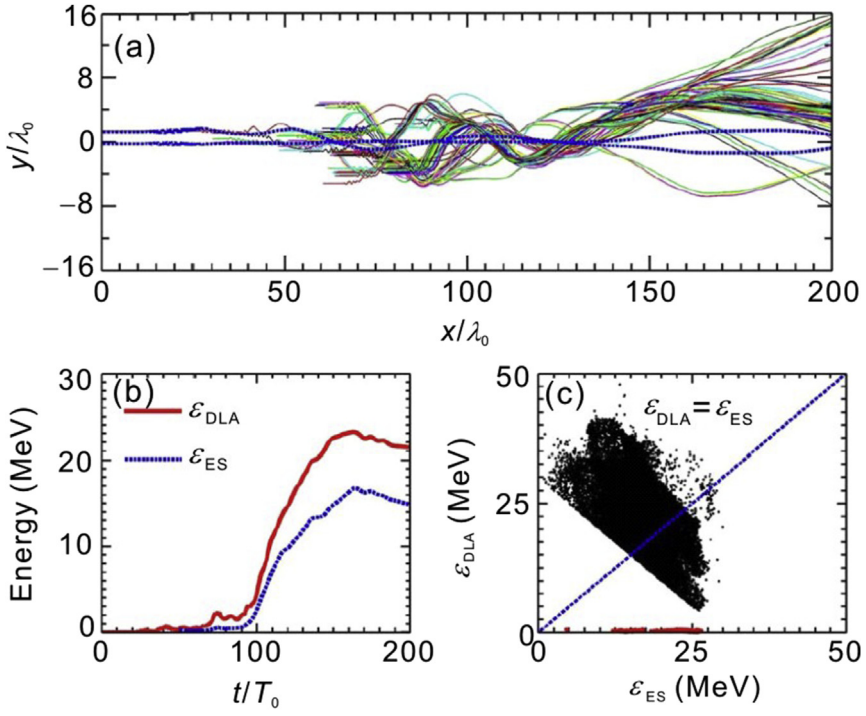

Fig. 1. (a) Trajectories of traced electrons with Ar (solid lines) and He (dashed blue lines). (b) Energy gain from DLA (red solid line) and ES field (blue line) for a traced electron. (c) Energy gain from DLA versus that from ES field with each point denotes a traced electron.

responsible for the bright betatron radiation with critical energy of 15 keV. However, our PIC simulations show that the potential of this second electron bunch is enormous. By using a 144 TW laser system with energy $E_L = 8.6$ J, pulse duration $\tau_0 = 60$ fs and $1/e^2$ spot size $w_0 = 18$ μm, the critical energy of the radiation could be boosted to 1.2 MeV [18]. Fig. 2 shows the evolution of electron density distribution. At the early stage the injection of monochromatic electron bunch is stable just as it should be. This self-injected electron bunch has a small oscillation amplitude of 1 μm. As the interaction goes on, the laser intensity increases due to the self-focusing and self-steepening of the laser pulse which then leads to increase of the plasma wavelength. This stretching of the bubble causes the oscillation and distortion of the bubble. Soon the bubble breaks at its rear where much larger electron density is accumulated from the bubble sheath, causing continuous injection with large initial transverse oscillation amplitude. When the laser pulse duration reduces to a few cycles, the carrier envelop effect dominates instead of the ponderomotive force. The plasma responds asymmetrically to the laser pulse, causing transverse oscillation of the bubble structure. The oscillation of the bubble enlarges the amplitude of the electron oscillation and further increases the laser hosing instability. This process results in a second electron bunch with energy ~2 GeV and oscillation amplitude 9 μm. The critical energy from this electron bunch is boosted to 1.2 MeV and the emitted photon number is ~10^{11}. Fig. 3 shows the emission spectra of the two electron bunch.

Experiment with similar parameters in our simulation has been demonstrated by scientists from South Korea, the experimental results evidently support our simulation results [50]. Such a gamma ray source based on a compact 100 TW class laser system will enable nuclear physics application in a university scale laboratory.

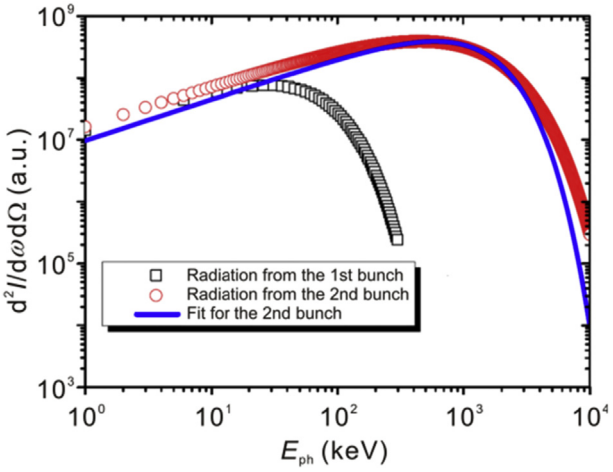

Fig. 3. Spectra of betatron radiation from the first (black squares) electron bunch and the second (red circles) continuously injected electron bunch. The blue solid line is a synchrotron fitting for the radiation of the second bunch.

5. Enhancing betatron radiation via ionization injection

Another new scheme is also demonstrated to enhance the betatron radiation by enabling the ionization injection of nitrogen [19]. The experiment was carried out with a 100 TW laser system at the Key Laboratory for Laser Plasmas at Shanghai Jiao Tong University, and the laser pulse of $\tau_0 = 40$ fs pulse duration and $E_L = 3$ J energy was focused by an $f/20$ OAP to a $1/e^2$ spot size $w_0 = 21$ μm leading to a normalized vector potential $a_0 = 2.2$. By using a 1.2 mm × 10 mm rectangular nozzle and pure nitrogen gas, electron beam peaked at 320 MeV with beam charge of 40 pC was obtained. The betatron radiation is fitted with the synchrotron radiation spectrum, giving a critical energy of 75 keV.

23 November 2023 14:53:30

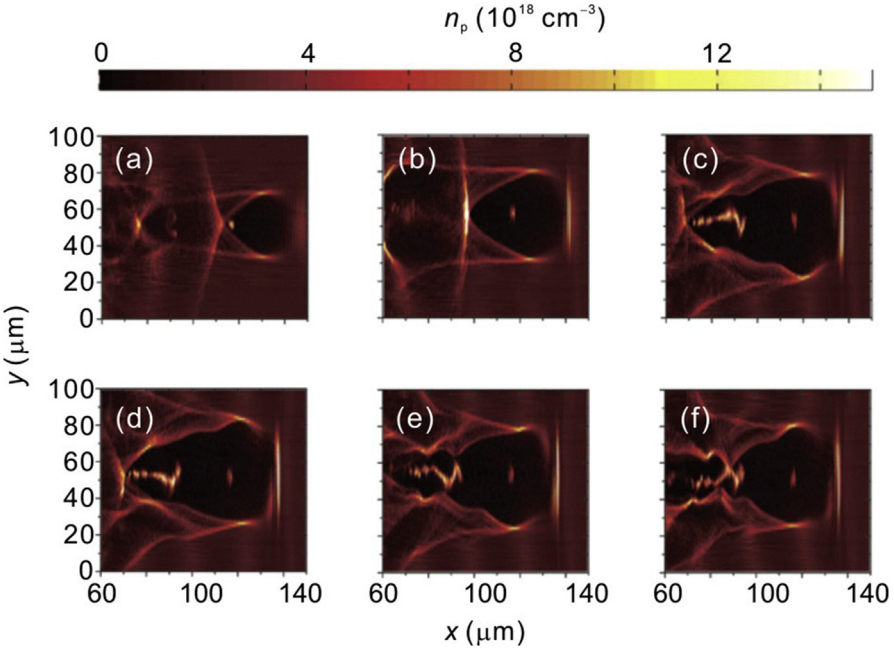

Fig. 2. Evolution of electron density distribution at (a) $t = 3.3$ ps, (b) $t = 20.9$ ps, (c) $t = 27.5$ ps, (d) $t = 28.4$ ps, (e) $t = 29.0$ ps, (f) $t = 30.0$ ps.

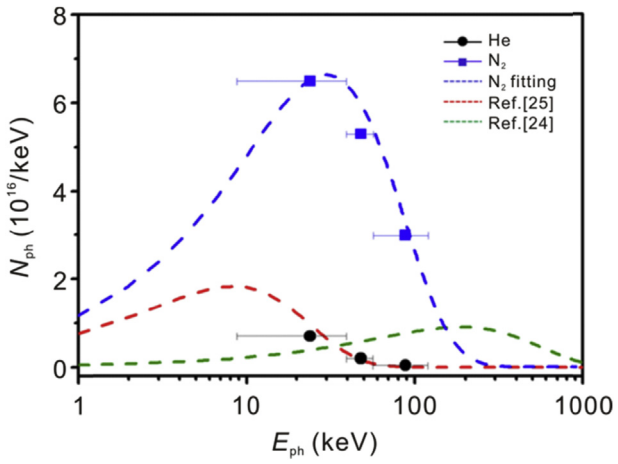

Fig. 4. Spectrum for resonantly enhanced betatron radiation vie ionization injection (blue squares), synchrotron fitting (blue dashed line). Self-injection results (black circles from this experiment with helium gas, red dashed line from Ref. [25] and green dashed line from Ref. [24]) are plotted as comparison.

The total emitted photon number is 8×10^8 and the photon number with energy higher than 110 keV is more than 1×10^8. The photon yield is ten times higher than the case with helium gas which is dominated by self-injection.

To reveal the physics of this enhancement, two-dimensional PIC simulation was performed. The simulation results suggest that the enhancement of the betatron X-ray yield and energy was resulted from "fast" ionization injection, which enabled the electrons to be quickly accelerated to the driving laser region for stimulating betatron resonance. At the resonant region, the oscillation amplitude increased to 10 μm which led to radiation enhancement. Fig. 4 shows the comparison of the current source's data with previous results [24,25].

6. Conclusion and perspectives

In this article we have briefly reviewed the laser plasma accelerator based betatron radiation sources and the relativistic Thomson backscattering (inverse Compton scattering) sources in the framework of classical electrodynamics. The synchrotron radiation model was adopted to develop the radiation properties. Realistic laser and plasma parameters were used to evaluate the performance of the sources. Both betatron and ICS sources hold the capability to deliver collimated intense gamma rays with pulse duration similar with the drive laser pulse, i.e., 20–40 fs. Together with the micrometer scale source size, the peak brightness of these sources is comparable to that of the third generation synchrotron sources. We have proposed a new method to boost the ICS source with a plasma mirror into higher nonlinearity level, i.e., higher photon energy and flux. We have also summarized our recent progress in enhancing the betatron radiation. By using a clustering gas jet, stimulating the hosing evolution as well as triggering the resonance between the ionization injected electron with the drive laser pulse, the radiation was enhanced with higher photon energy and flux. Further efforts could be done to improve the stability of these sources. With these methods and rapid development in high power high repetition rate lasers, the average photon flux could be improved by orders of magnitude, which will make these sources powerful tools for various applications.

Conflict of interest

The authors declare no competing financial interest.

Acknowledgement

This work was supported by the National Basic Research Program of China (2013CBA01500), the National Key Scientific Instrument and Equipment Development Project (2012YQ120047), the National Natural Science Foundation of China (11334013, 11421064, 11374210, and 11305185) and the CAS Key Program (KGZD-EW-T05).

References

[1] E. Eggl, S. Schleede, M. Bech, K. Achterhold, R. Loewen, et al., X-ray phase-contrast tomography with a compact laser-driven synchrotron source, Proc. Natl. Acad. Sci. U.S.A. 112 (2015), https://doi.org/10.1073/pnas.1500938112.
[2] K. Achterhold, M. Bech, S. Schleede, G. Potdevin, R. Ruth, et al., Monochromatic computed tomography with a compact laser-driven X-ray source, Sci. Rep. 3 (2013) 1313, https://doi.org/10.1038/srep01313.
[3] H.-P. Schlenvoigt, K. Haupt, A. Debus, F. Budde, O. Jäckel, et al., A compact synchrotron radiation source driven by a laser-plasma wakefield accelerator, Nat. Phys. 4 (2007) 130–133, https://doi.org/10.1038/nphys811.
[4] V. Malka, Laser plasma accelerators, Phys. Plasmas 55501 (2013), https://doi.org/10.1063/1.3695389.
[5] E. Esarey, C.B. Schroeder, W.P. Leemans, Physics of laser-driven plasma-based electron accelerators, Rev. Mod. Phys. 81 (2009), https://doi.org/10.1103/RevModPhys.81.1229.
[6] J.M. Tajima, T. Dawson, Laser electron accelerator, Phys. Rev. Lett. 43 (1979) 267–270.
[7] W. Lu, M. Tzoufras, C. Joshi, Generating multi-GeV electron bunches using single stage laser wakefield acceleration in a 3D nonlinear regime, Phys. Rev. Accel. Beams 61301 (2007) 1–12, https://doi.org/10.1103/PhysRevSTAB.10.061301.
[8] A. Pukhov, J. Meyer-ter-Vehn, Laser wake field acceleration: the highly non-linear broken-wave regime, Appl. Phys. B Lasers Opt. 74 (2002) 355–361, https://doi.org/10.1007/s003400200795.
[9] X. Wang, R. Zgadzaj, N. Fazel, Z. Li, S.A. Yi, et al., Quasi-monoenergetic laser-plasma acceleration of electrons to 2 GeV, Nat. Commun. 4 (2013) 1988, https://doi.org/10.1038/ncomms2988.
[10] K. Nakamura, C.G.R. Geddes, W.P. Leemans, B. Nagler, A.J. Gonsalves, et al., GeV electron beams from a centimetre-scale accelerator, Nat. Phys. 2 (2006) 9–12, https://doi.org/10.1038/nphys418.
[11] C. Ding, W. Xiong, T. Fan, D.D. Hickstein, T. Popmintchev, et al., High flux coherent super-continuum soft X-ray source driven by a single-stage, 10 mJ, Ti:sapphire amplifier-pumped OPA, Opt. Express 22 (2014) 6194, https://doi.org/10.1364/OE.22.006194.
[12] L.M. Chen, M. Kando, M.H. Xu, Y.T. Li, J. Koga, et al., Study of X-ray emission enhancement via a high-contrast femtosecond laser interacting with a solid foil, Phys. Rev. Lett. 100 (2008) 1–4, https://doi.org/10.1103/PhysRevLett.100.045004.
[13] L.M. Chen, W.M. Wang, M. Kando, L.T. Hudson, F. Liu, et al., High contrast femtosecond laser-driven intense hard X-ray source for imaging

23 November 2023 14:53:30

application, Nucl. Instrum. Methods Phys. Res. Sect. A Accel. Spectrom. Detect. Assoc. Equip. 619 (2010) 128−132, https://doi.org/10.1016/j.nima.2009.11.048.
[14] M. Li, K. Huang, L. Chen, W. Yan, M. Tao, et al., Laser-driven powerful kHz hard X-ray source, Radiat. Phys. Chem. (2016) 1−5, https://doi.org/10.1016/j.radphyschem.2016.01.042.
[15] Y. Glinec, J. Faure, L. Le Dain, S. Darbon, T. Hosokai, et al., High-resolution γ-ray radiography produced by a laser-plasma driven electron source, Phys. Rev. Lett. 94 (2005) 1−4, https://doi.org/10.1103/PhysRevLett.94.025003.
[16] L.M. Chen, W.C. Yan, D.Z. Li, Z.D. Hu, L. Zhang, et al., Bright betatron X-ray radiation from a laser-driven-clustering gas target, Sci. Rep. 3 (2013) 1912, https://doi.org/10.1038/srep01912.
[17] W. Yan, L. Chen, D. Li, L. Zhang, N.A.M. Hafz, et al., Concurrence of monoenergetic electron beams and bright X-rays from an evolving laser-plasma bubble, Proc. Natl. Acad. Sci. U.S.A. 111 (2014) 5825−5830, https://doi.org/10.1073/pnas.1404336111.
[18] Y. Ma, L. Chen, D. Li, W. Yan, K. Huang, et al., Generation of femtosecond gamma-ray bursts stimulated by laser-driven hosing evolution, Sci. Rep. 6 (2016), https://doi.org/10.1038/srep30491.
[19] K. Huang, L.M. Chen, Y.F. Li, D.Z. Li, M.Z. Tao, et al., Resonantly Excited Betatron Hard X-rays from Ionization Injected Electron Beam in a Laser Plasma Accelerator, 2015, pp. 1−5, https://doi.org/10.1038/srep27633.
[20] J.D. Jackson, Classical Electrodynamics, third ed., Wiley, New York, 2001.
[21] S. Corde, K. Ta Phuoc, G. Lambert, R. Fitour, V. Malka, et al., Femtosecond X rays from laser-plasma accelerators, Rev. Mod. Phys. 85 (2013) 1−48, https://doi.org/10.1103/RevModPhys.85.1.
[22] E. Esarey, B.A. Shadwick, P. Catravas, W.P. Leemans, Synchrotron radiation from electron beams in plasma-focusing channels, Phys. Rev. E − Stat. Nonlinear Soft Matter Phys. 65 (2002) 1−15, https://doi.org/10.1103/PhysRevE.65.056505.
[23] A. Rousse, K. Ta Phuoc, R. Shah, A. Pukhov, E. Lefebvre, et al., Production of a keV X-ray beam from synchrotron radiation in relativistic laser-plasma interaction, Phys. Rev. Lett. 93 (2004) 1−4, https://doi.org/10.1103/PhysRevLett.93.135005.
[24] S. Cipiccia, M.R. Islam, B. Ersfeld, R.P. Shanks, E. Brunetti, et al., Gamma-rays from harmonically resonant betatron oscillations in a plasma wake, Nat. Phys. 7 (2011) 867−871, https://doi.org/10.1038/nphys2090.
[25] S. Kneip, C. McGuffey, J.L. Martins, S.F. Martins, C. Bellei, et al., Bright spatially coherent synchrotron X-rays from a table-top source, Nat. Phys. 6 (2010) 980−983, https://doi.org/10.1038/nphys1789.
[26] F. Albert, A.G.R. Thomas, S.P.D. Mangles, S. Banerjee, S. Corde, et al., Laser wakefield accelerator based light sources: potential applications and requirements, Plasma Phys. Control. Fusion 56 (2014) 84015, https://doi.org/10.1088/0741-3335/56/8/084015.
[27] J. Wenz, S. Schleede, K. Khrennikov, M. Bech, P. Thibault, et al., Quantitative X-ray phase-contrast microtomography from a compact laser-driven betatron source, Nat. Commun. 6 (2015) 7568, https://doi.org/10.1038/ncomms8568.
[28] F. Albert, A.G.R. Thomas, Applications of laser wakefield accelerator-based light sources, Plasma Phys. Control. Fusion 58 (2016) 103001, https://doi.org/10.1088/0741-3335/58/10/103001.
[29] C. Yu, R. Qi, W. Wang, J. Liu, W. Li, et al., Ultrahigh brilliance quasi-monochromatic MeV γ-rays based on self-synchronized all-optical Compton scattering, Sci. Rep. 6 (2016) 29518, https://doi.org/10.1038/srep29518.
[30] S. Kneip, S.R. Nagel, C. Bellei, N. Bourgeois, A.E. Dangor, et al., Observation of synchrotron radiation from electrons accelerated in a petawatt-laser-generated plasma cavity, Phys. Rev. Lett. 100 (2008) 1−4, https://doi.org/10.1103/PhysRevLett.100.105006.
[31] J. Ferri, X. Davoine, S.Y. Kalmykov, A. Lifschitz, Electron acceleration and generation of high-brilliance X-ray radiation in kilojoule, subpicosecond laser-plasma interactions, Phys. Rev. Accel. Beams 19 (2016) 101301, https://doi.org/10.1103/PhysRevAccelBeams.19.101301.
[32] F.V. Hartemann, D.J. Gibson, W.J. Brown, A. Rousse, K.T. Phuoc, et al., Compton scattering X-ray sources driven by laser wakefield acceleration, Phys. Rev. Spec. Top. − Accel. Beams 10 (2007) 1−8, https://doi.org/10.1103/PhysRevSTAB.10.011301.
[33] E. Esarey, S.K. Ride, P. Sprangle, Nonlinear Thomson scattering of intense laser pulses from beams and plasmas, Phys. Rev. E 48 (1993) 3003−3021, https://doi.org/10.1103/PhysRevE.48.3003.
[34] S.K. Ride, E. Esarey, M. Baine, Thomson scattering of intense lasers from electron beams at arbitrary interaction angles, Phys. Rev. E 52 (1995) 5425−5442, https://doi.org/10.1103/PhysRevE.52.5425.
[35] K. Khrennikov, J. Wenz, A. Buck, J. Xu, M. Heigoldt, et al., Tunable all-optical quasimonochromatic Thomson X-ray source in the nonlinear regime, Phys. Rev. Lett. 114 (2015) 1−5, https://doi.org/10.1103/PhysRevLett.114.195003.
[36] N.D. Powers, I. Ghebregziabher, G. Golovin, C. Liu, S. Chen, et al., Quasi-monoenergetic and tunable X-rays from a laser-driven Compton light source, Nat. Photonics 8 (2013) 28−31, https://doi.org/10.1038/nphoton.2013.314.
[37] G. Sarri, D.J. Corvan, W. Schumaker, J.M. Cole, A. Di Piazza, et al., Ultrahigh brilliance multi-MeV γ-ray beams from nonlinear relativistic thomson scattering, Phys. Rev. Lett. 113 (2014) 1−5, https://doi.org/10.1103/PhysRevLett.113.224801.
[38] K. Ta Phuoc, S. Corde, C. Thaury, V. Malka, A. Tafzi, et al., All-optical Compton gamma-ray source, Nat. Photonics 6 (2012) 308−311, https://doi.org/10.1038/nphoton.2012.82.
[39] H.E. Tsai, X. Wang, J.M. Shaw, Z. Li, A.V. Arefiev, et al., Compact tunable Compton X-ray source from laser-plasma accelerator and plasma mirror, Phys. Plasmas 22 (2015), https://doi.org/10.1063/1.4907655.
[40] H. Vincenti, S. Monchocé, S. Kahaly, G. Bonnaud, P. Martin, et al., Optical properties of relativistic plasma mirrors, Nat. Commun. 5 (2014) 3403, https://doi.org/10.1038/ncomms4403.
[41] M. Nakatsutsumi, A. Kon, S. Buffechoux, P. Audebert, J. Fuchs, et al., Fast focusing of short-pulse lasers by innovative plasma optics toward extreme intensity, Opt. Lett. 35 (2010) 2314−2316, https://doi.org/10.1364/OL.35.002314.
[42] A. Di Piazza, C. Müller, K.Z. Hatsagortsyan, C.H. Keitel, Extremely high-intensity laser interactions with fundamental quantum systems, Rev. Mod. Phys. 84 (2012) 1177−1228, https://doi.org/10.1103/RevModPhys.84.1177.
[43] A.I. Titov, Cumulative multi-photon processes in electron-laser Compton scattering, Proc. Sci. (2015) 1−16.
[44] J. Gao, Thomson scattering from ultrashort and ultraintense laser pulses, Phys. Rev. Lett. 93 (2004) 18−21, https://doi.org/10.1103/PhysRevLett.93.243001.
[45] O.E. Vais, S.G. Bochkarev, V.Y. Bychenkov, Nonlinear Thomson scattering of a relativistically strong tightly focused ultrashort laser pulse, Plasma Phys. Rep. 42 (2016) 818−833, https://doi.org/10.1134/S1063780X16090105.
[46] A. Oguz Er, J. Chen, P.M. Rentzepis, Ultrafast time resolved X-ray diffraction, extended X-ray absorption fine structure and X-ray absorption near edge structure, J. Appl. Phys. 112 (2012), https://doi.org/10.1063/1.4738372.
[47] A. Krol, A. Ikhlef, J.C. Kieffer, D.A. Bassano, C.C. Chamberlain, et al., Laser-based microfocused X-ray source for mammography: feasibility study, Med. Phys. 24 (1997) 725−732, https://doi.org/10.1118/1.597993.
[48] S. Gales, D.L. Balabanski, F. Negoita, O. Tesileanu, C.A. Ur, et al., New frontiers in nuclear physics with high-power lasers and brilliant monochromatic gamma beams, Phys. Scr. 91 (2016) 93004, https://doi.org/10.1088/0031-8949/91/9/093004.
[49] L.M. Chen, J.J. Park, K.H. Hong, J.L. Kim, J. Zhang, et al., Emission of a hot electron jet from intense femtosecond-laser-cluster interactions, Phys. Rev. E − Stat. Nonlinear Soft Matter Phys. 66 (2002) 17−20, https://doi.org/10.1103/PhysRevE.66.025402.
[50] J.H. Jeon, K. Nakajima, H.T. Kim, Y.J. Rhee, V.B. Pathak, et al., Measurement of angularly dependent spectra of betatron gamma-rays from a laser plasma accelerator with quadrant-sectored range filters, Phys. Plasmas 23 (2016), https://doi.org/10.1063/1.4956447.

23 November 2023 14:53:30